Polar Geosci., **18**, 114–129, 2005

Geochemistry of the pre/syn-metamorphic granite in the Ongul Islands, East Antarctica

Yoshinobu Kawano[1]*, Akihiro Meno[2], Naoko Nishi[3] and Hiroo Kagami[4]

[1]*Faculty of Culture and Education, Saga University, Honjo 1, Saga 840-8502*
[2]*Karatsu 5th Junior High School, Watada, Karatsu 847-0075*
[3]*Yamagata City, Yamagata 990-2331*
[4]*Graduate School of Science and Technology, Niigata University, Ikarashi, Niigata 950-2181*
**Corresponding author. E-mail: kawanoy@cc.saga-u.ac.jp*

(Received March 10, 2005; Accepted July 15, 2005)

Abstract: Latest Proterozoic to Early Paleozoic pre/syn- and post-metamorphic granites occur in the Lützow-Holm Complex (LHC), East Antarctica. The pre/syn-metamorphic granites in the Ongul Islands consist of biotite hornblende (BH) granite and garnet biotite hornblende (GBH) granite. The Rb-Sr whole rock isochron age of 580±23 Ma with an initial $^{87}Sr/^{86}Sr$ ratio of 0.70784±0.00059 is obtained from the BH granite. This age is slightly older than SHRIMP U-Pb zircon and CHIME monazite metamorphic ages (520–550 Ma) from the complex. The BH granite has lower aluminum saturation index than the GBH granite. The pre/syn-metamorphic granites have a wide variation of εSr and εNd values at 580 m.y. before the present, and the BH granite has lower εSr_{580Ma} and higher εNd_{580Ma} values than the GBH granite. One end of the variations in the ε diagram is close to the values of the mafic to intermediate metamorphic rocks in the island; the other is close to those of the old continental crust. These geochemical and isotopic features suggest that the PSMGs were originated by mixing between magma derived from mafic to intermediate metamorphic rocks and old continental crust.

key word: granite, geochemistry, isotope, Ongul Islands, Lützow-Holm Complex

1. Introduction

Latest Proterozoic to Early Paleozoic granites are distributed in the Lützow-Holm Complex (LHC), which is a Cambrian high-grade metamorphic terrane having U-Pb metamorphic ages of 520–550 Ma (Shiraishi *et al*., 1994, 2003). Ajishi *et al*. (2004) categorized the granites into pre/syn- and post-metamorphic granites on the basis of the mode of occurrence as follows. Pre/syn-metamorphic granites show ambiguous contacts and gneissose structures, and are deformed. In contrast, post-metamorphic granites are characterized by sharp intrusive contacts and by crosscutting the layered gneissose structure of the metamorphic rocks, and are unmetamorphosed and not distinctively deformed.

Shimura *et al*. (1998) investigated pre/syn-metamorphic granite in Breidvågnipa and reported a 576±39 Ma Rb-Sr whole rock isochron age, which is slightly older

than the peak metamorphic age (540 Ma) of the LHC. On the other hand, post-metamorphic granites are exposed in the Oku-iwa Rock and Kasumi Rock of the complex, and their Rb-Sr whole rock isochron ages have been dated to be 485±50 Ma and 492±23 Ma, respectively (Nishi *et al*., 2002; Ajishi *et al*., 2004). Petrogenesis of both pre/syn- and post-metamorphic granites is interesting, because they potentially provide tectonic and magma processes of high-grade LHC in the context of the Pan-African event or the formation of the Gondwana Super Continent (Windly, 1995).

In this paper, we report the major and trace element chemical compositions, and Sr and Nd isotopic compositions, of the pre/syn-metamorphic granites in the Ongul Islands, and estimate source materials on the basis of the geochemical data.

2. Outline of geology

The Ongul Islands belong to the granulite facies terrane in the LHC (Hiroi *et al*., 1991), and are underlain mainly by pyroxene gneiss, hornblende gneiss, and garnet gneiss with mafic to ultramafic interlayers (*e.g*., Kizaki, 1962, 1964; Hiroi and Onuki, 1985; Ishikawa *et al*., 1994) (Fig. 1). The metamorphic rocks commonly show compo-

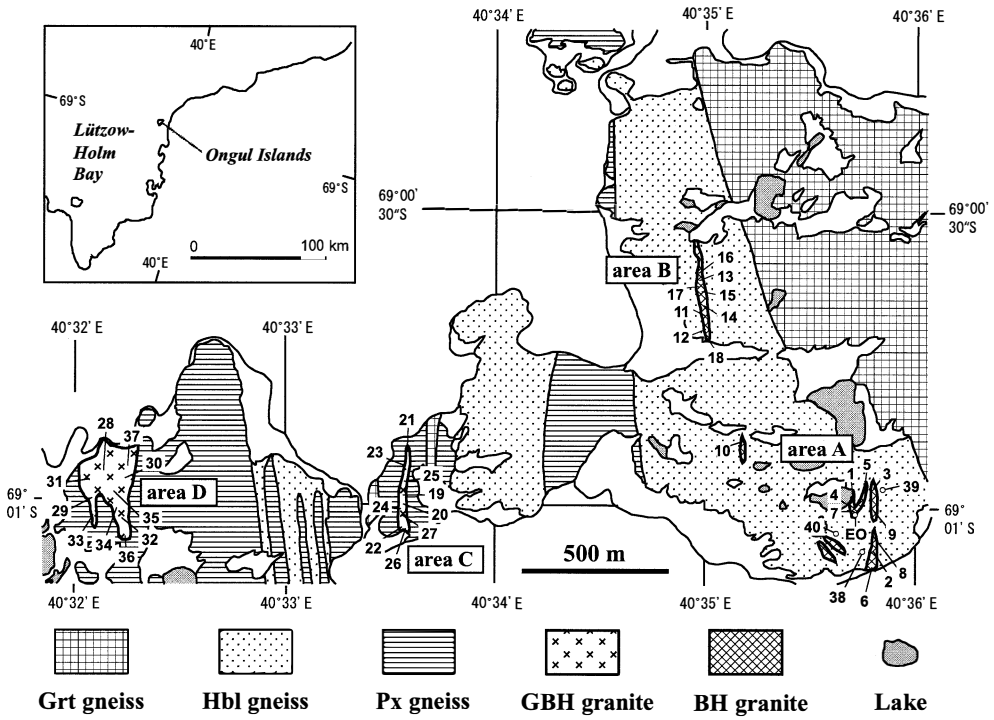

Fig. 1. Geological map of a part of the Ongul Islands simplified from Ishikawa et al. (1994). Grt, garnet; Hbl, hornblende; Px, pyroxene; GBH, garnet biotite hornblende; BH, biotite hornblende. EO is sampling site of 80EO125 discussed by Shibata et al. (1985, 1986). Numbers indicate sampling sites for analyzed rocks of the same number in Table 1.

sitional layering, generally parallel to the lithological boundaries. The regional strikes of these foliations are N-S to NNW-SSE with 60–25°E dips (Ishikawa *et al*., 1994). An isoclinal fold in the East Ongul Island about 1 km in wavelength is a prominent megascopic structure. The general strikes of the foliation and fold axis are approximately N20°W, and dip 10°E in the eastern limb of the fold and 40°E in the western limb (Yanai *et al*., 1974a, b).

The pre/syn-metamorphic granites (abbreviated to PSMG hereafter) mainly occur in four areas, A to D, as shown in Fig. 1 (Yanai *et al*., 1974a, b; Ishikawa *et al*., 1994). All granites have foliations, which coincide with those of metamorphic rocks including pyroxene gneiss, hornblende gneiss and garnet gneiss, and show ambiguous and locally sharp contacts.

Medium-grained pyroxene gneiss is the most dominant rock type of intermediate composition throughout the Ongul Islands. The main constituent minerals are feldspars, quartz, clinopyroxene, orthopyroxene, hornblende and accessory magnetite, apatite and zircon (Ishikawa *et al*., 1994). Hornblende gneiss intercalates mainly pyroxene gneiss in the central part of East Ongul Island. The gneisses consist of hornblende, biotite, plagioclase, K-feldspar and quartz, and accessory ilmenite, hematite, magnetite, apatite and zircon. Massive granoblastic garnet gneiss is intercalated with pyroxene gneiss. The main constituent minerals are garnet, clinopyroxene, plagioclase, K-feldspar and quartz. There are many pegmatite dikes several tens to a few meters wide (Kizaki, 1964).

Age data from the Ongul Islands have been published by many authors. K-Ar biotite and hornblende ages of biotite hornblende gneiss in East Ongul Island are 480±15 Ma and 502±15 Ma, respectively (Shibata *et al*., 1985). Garnet biotite gneiss from the island yielded CHIME monazite ages of 533±10 Ma and 537±9 Ma (Asami *et al*., 1997). Garnet biotite gneiss in West Ongul Island also has been dated at 532±6 Ma by the SHRIMP U-Pb method (Shiraishi *et al*., 1992). Shibata *et al*. (1985) reported an Rb-Sr mineral isochron age of 482±10 Ma for a granitic rock in East Ongul Island, and Shibata *et al*. (1986) obtained an Rb-Sr whole rock isochron age of 683±13 Ma for metamorphic rocks including the gneissose granite in this study.

3. Descriptions of the PSMGs

The granitic rocks in areas A and B consist of granite with mafic mineral assemblages of hornblende±biotite, while those in areas C and D consist of granite and alkali feldspar granite with mafic mineral assemblages of hornblende±biotite±garnet or, rarely, biotite+garnet without hornblende (Fig. 2). The former and latter are named biotite hornblende granite (BH granite) and garnet biotite hornblende granite (GBH granite), respectively.

3.1. BH granite

BH granites in area A are mainly medium-grained (~6 mm) with foliations and gradual contact (Fig. 3A). In particular, an isolated body in the western part of this area is distinctively deformed and shows ambiguous contact. The regional strikes of these foliations are N-S to NNW-SSE with 60–37°E dips, which are consistent with the

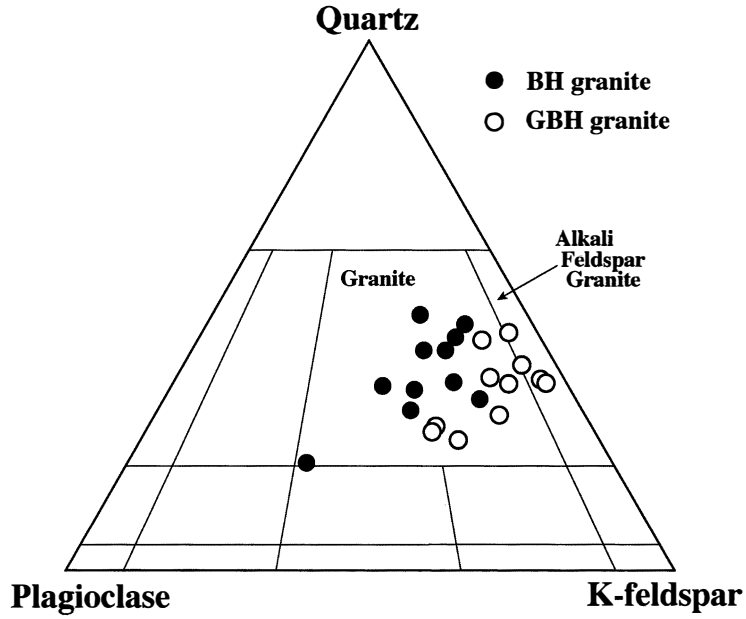

Fig. 2. Modal quartz–plagioclase–K-feldspar triangular diagram. Classification boundaries are after IUGS (1973).

gneissose structure of the surrounding metamorphic rocks. The constituent minerals are K-feldspar (modal compositions, 25–50%), quartz (17–39%), plagioclase (15–42%), and hornblende (1.2–12%) with or without biotite (0.1–1.3%), with sphene, zircon, apatite, pyrite and ilmenite as accessory minerals (Fig. 4A). K-feldspar and quartz are subhedral to anhedral, up to 6 mm in diameter. Plagioclase is subhedral, up to 5 mm in diameter; partly corroded grains are common. Anhedral tiny clinopyroxene inclusions occasionally occur in plagioclase. Hornblende is euhedral to subhedral, sometimes containing anhedral to subhedral grains of quartz, with K-feldspar and plagioclase as inclusions. Ilmenite occasionally includes small magnetite grains.

BH granites in area B have relatively sharp contact with the surrounding rocks (Fig. 3B). The granites are medium-grained (~6 mm) rocks without chilled margins. The rocks have foliations trending NNW-SSE with 53–32°E dips. The constituent minerals are quartz (39–45%), K-feldspar (32–42%), plagioclase (11–16%) and hornblende (1.0–5.6%) (Fig. 4B). Accessory minerals are biotite, sphene, apatite, zircon, ilmenite and pyrite with or without clinopyroxene. Quartz and K-feldspar are subhedral to anhedral, up to 6 mm in diameter. Plagioclase and hornblende are subhedral and partly corroded. The hornblende includes small quartz, K-feldspar and plagioclase.

3.2. GBH granite

GBH granites in area C have foliations with strikes of N-S to NNW-SSE, and 60–37°E dips. The boundary between the GBH granite and pyroxene gneiss is distinct

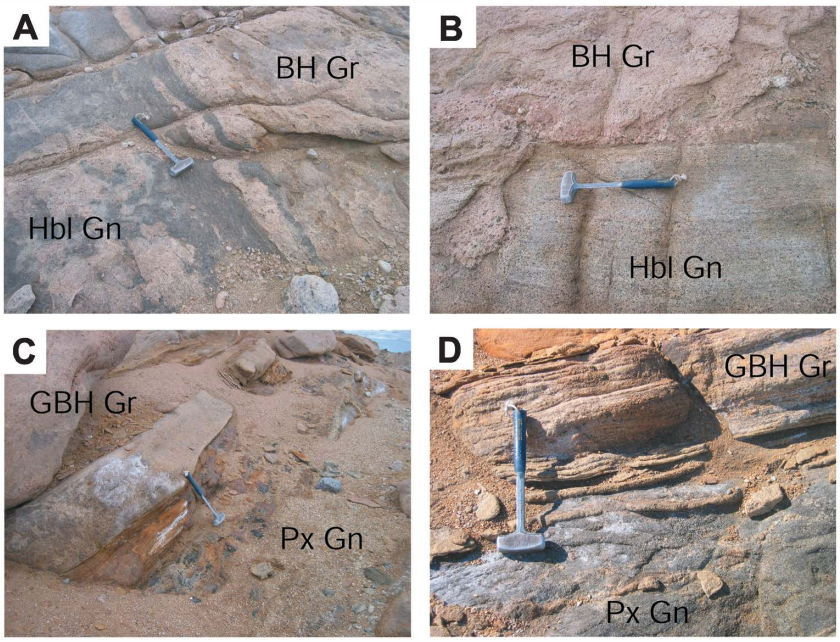

Fig. 3. Photographs showing mode of occurrence of the PSMGs. A–D, Relationships between granites and gneissose rocks in areas A–D. Gn, gneiss; Gr, granite; other abbreviations are the same as those in Fig. 1.

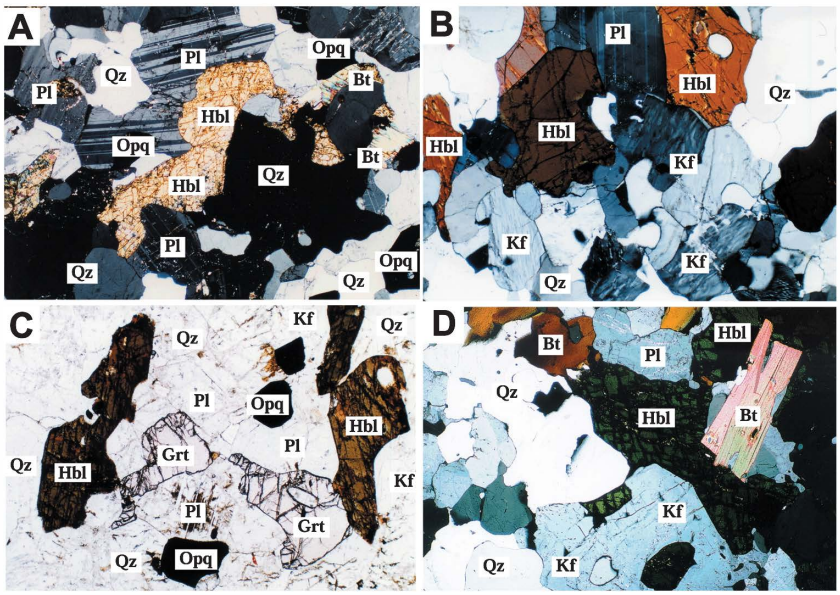

Fig. 4. Microphotographs of the PSMGs (width=2.5 mm). A and B, microphotographs of BH granite in areas A and B, respectively (crossed nicols); C and D, microphotographs of the GBH granite in areas C and D, respectively (crossed nicols). Qz, quartz; Pl, plagioclase; Kf, K-feldspar; Opq, opaque minerals; other abbreviations are the same as those in Fig. 1.

(Fig. 3C). The constituent minerals are K-feldspar (45–58%), quartz (27–34%), plagioclase (3–24%), hornblende (4.5–6.0%) and garnet (1.1–1.8%), with biotite, apatite, zircon, sphene, ilmenite and pyrite as accessories. Unusual coexistence of hornblende and garnet is seen (Fig. 4C). K-feldspar and quartz are anhedral to subhedral, up to 5 mm in diameter. Most plagioclase and hornblende is subhedral and corroded.

Granites in area D in the northeastern part of West Ongul Island (Fig. 1; Fig. 3D) show foliations with strike generally N19°E to N8°W and 50–29°E dips. The constituent minerals are K-feldspar (47–55%), quartz (23–43), plagioclase (6–25%), biotite (0.1–5.4%) and hornblende (0.1–5.0%) (Fig. 4D); though hornblende and/or biotite is sometimes absent. Accessory minerals are garnet, apatite, zircon, sphene, ilmenite and pyrite. K-feldspar, plagioclase and quartz are subhedral to anhedral, up to 6 mm in diameter. Biotite is usually accompanied by hornblende and is altered to secondary chlorite. Hornblende and plagioclase are partly corroded. Tiny garnet inclusions occasionally occur in feldspars.

4. Bulk chemical composition

Major and trace elements of forty rock samples were analyzed by the X-ray fluorescence method on glass fusion discs at Fukuoka University of Education and the Analytical Research Center for Experimental Sciences, Saga University. FeO and loss on ignition (L.O.I.) were determined by wet chemical analysis at Saga University. Bulk chemical compositions of the PSMGs are listed in Table 1 with three leucosomes in the hornblende gneiss in area A. The leucosomes are analyzed to determine the geochemical behavior of materials which originated from hornblende gneiss, and for the sake of comparison with the PSMGs. Localities of analyzed samples are shown in Fig. 1.

Silica contents of the BH granite and GBH granite are nearly the same. The aluminum saturation index (ASI) of the BH granite ranges from 0.80 to 1.04 and most of the rocks indicate metaluminous signature, whereas that of the GBH granite varies from 0.94 to 1.12 (Table 1).

Harker plots for major and trace elements are shown in Figs. 5 and 6. TiO_2, Al_2O_3, FeO^*, MnO, CaO, Nb, V, Y and Zn contents of both the BH and GBH granites are negatively correlated against SiO_2 contents, and correlations of other elements are scattered. Abundances of TiO_2, MgO, Cr, Sr and V of the BH granite are significantly greater than those of the GBH granite, whereas the GBH granite shows higher Al_2O_3, Na_2O, K_2O and Rb contents in comparison with the BH granite.

Leucosomes in the hornblende gneiss are characterized by higher Al_2O_3, K_2O, Ba and Sr contents, and lower TiO_2, FeO^*, MnO, Zn and Zr contents, than those of the PSMGs. Their Al_2O_3, MgO and Rb contents show similar behavior with those of the GBH granites, but Sr, V and Y contents are similar to those of the BH granites. Geochemical features of leucosomes from hornblende gneiss are distinctly different from those of the PSMGs.

Table 1. Major (wt%) and trace

No.	1	2	3	4	5	6	7	8	9	10
	BH granite in area A									
Sp. No.	**95020202**	**95020204**	**95020206**	**95020203**	**03020513**	**95020101**	**03020603**	**95020205**	**95020201**	**03020512**
SiO_2	65.62	69.37	69.45	69.56	69.56	69.62	70.14	70.17	71.80	74.03
TiO_2	0.80	0.70	0.65	0.71	0.88	0.61	0.67	0.54	0.55	0.14
Al_2O_3	14.20	13.10	13.36	12.63	14.28	13.22	12.01	13.47	12.76	14.29
Fe_2O_3	3.85	3.81	3.31	3.37	1.16	3.06	1.73	2.83	2.63	0.22
FeO	2.53	2.26	1.88	2.06	1.61	2.48	3.20	1.63	1.90	0.48
MgO	0.63	0.49	0.50	0.59	0.58	0.52	1.74	0.50	0.47	0.13
MnO	0.09	0.07	0.06	0.07	0.04	0.07	0.08	0.05	0.05	0.01
CaO	2.88	2.04	1.78	2.28	2.11	2.05	3.83	1.68	1.42	1.50
Na_2O	3.32	2.73	2.54	2.13	3.32	2.90	2.41	2.62	2.56	3.31
K_2O	4.07	4.92	5.17	5.46	5.20	4.92	3.71	5.98	5.05	5.28
P_2O_5	0.11	0.12	0.11	0.12	0.12	0.09	0.28	0.09	0.07	0.02
L.O.I.	1.23	0.17	0.91	0.77	0.78	0.27	0.80	0.29	0.62	0.56
Total	99.33	99.77	99.71	99.74	99.64	99.82	100.60	99.86	99.90	99.96
Ba	693	797	856	781	1251	743	860	966	815	1483
Cr	6	17	15	15		19	36	17	6	
Cu			9	3						
Nb	45	28	37	25	11	23	15	21	30	2
Ni	22	21	24	21		18	10	20	24	
Rb	122	139	164	177	122	147	102	181	169	121
Sr	145	145	172	199	616	183	335	140	159	926
V	65	42	57	43	42	51	60	51	36	7
Y	71	57	75	61	37	52	136	52	69	13
Zn	436	340	244	135	52	264	89	317	171	3
Zr	377	358	404	324	404	288	223	299	427	97
ASI	0.94	0.97	1.03	0.93	0.96	0.96	0.80	0.97	1.04	1.03

No.	21	22	23	24	25	26	27	28	29	30
	GBH granite in area C									
Sp. No.	**95020308**	**95020304**	**95020307**	**03020505**	**03020504**	**03020506**	**95020305**	**95020407**	**95020402**	**03020307**
SiO_2	71.34	72.12	72.37	72.40	72.52	73.60	75.72	65.62	71.73	72.49
TiO_2	0.40	0.37	0.34	0.44	0.40	0.34	0.42	0.36	0.25	0.29
Al_2O_3	13.28	13.14	13.31	13.04	13.27	12.76	12.04	16.66	14.81	14.08
Fe_2O_3	1.44	0.85	1.42	1.98	1.65	1.35	0.33	1.77	0.42	0.28
FeO	2.09	2.43	1.69	2.06	1.98	1.79	1.41	2.19	1.41	1.43
MgO	0.33	0.33	0.29	0.18	0.13	0.15	0.42	0.32	0.45	0.56
MnO	0.06	0.04	0.04	0.07	0.04	0.02	0.02	0.03	0.03	0.01
CaO	1.61	1.38	1.16	1.50	1.47	1.30	1.40	1.84	1.19	0.64
Na_2O	2.51	2.72	2.62	2.90	2.30	2.80	2.18	3.96	3.40	2.29
K_2O	6.04	6.21	6.24	5.20	5.76	5.53	5.99	6.48	6.08	7.82
P_2O_5	0.04	0.03	0.03	0.05	0.05	0.05	0.04	0.07	0.07	0.20
L.O.I.	0.76	0.36	0.46	0.57	1.18	0.66	0.46	0.28	0.36	0.43
Total	99.91	99.98	99.97	100.38	100.75	100.34	100.42	99.58	100.20	100.53
Ba	1058	747	865	1108	1141	1035	1082	784	380	572
Cr	20	11	15	7			8	11	23	10
Cu								6		
Nb	36	24	25	28	24	18	25	27	10	7
Ni	25	20	24			1	29	25	26	2
Rb	230	190	210	187	183	182	221	144	220	329
Sr	171	132	128	127	135	229	226	231	140	115
V	23	29	13	42		19	27	22	14	35
Y	76	64	62	185	129	103	65	64	40	65
Zn	94	139	192	109	92	105	71	31	39	25
Zr	380	253	266	442	478	444	349	544	251	153
ASI	0.98	0.96	1.01	0.99	1.04	0.99	0.95	0.99	1.03	1.05

No, sample numbers in Fig. 1; ASI, aluminum saturation index.

(ppm) elements of the PSMGs.

11	12	13	14	15	16	17	18	19	20
BH granite in area B								GBH gr. in area C	
03020610	**95020508**	**95020301**	**95020303**	**95020302**	**03020614**	**03020616**	**03020608**	**95020306**	**03020507**
71.46	71.56	72.30	72.42	73.69	73.73	74.22	74.30	67.79	70.51
0.32	0.53	0.50	0.56	0.33	0.42	0.57	0.68	0.44	0.54
12.64	12.80	12.04	13.31	12.57	12.77	11.66	11.38	15.41	13.23
1.76	2.83	2.27	1.66	2.13	1.78	2.03	2.26	1.16	2.04
0.89	1.40	1.66	0.83	1.22	1.09	1.34	0.88	2.25	2.75
0.47	0.80	1.27	0.66	0.56	0.41	0.94	0.69	0.54	0.32
0.03	0.05	0.05	0.03	0.03	0.01	0.04	0.04	0.04	0.06
2.94	1.28	1.59	1.11	1.25	1.27	1.37	1.01	2.57	1.98
1.29	2.79	2.45	2.57	2.80	2.89	2.34	2.35	4.03	3.04
6.38	5.69	5.32	6.52	5.21	5.17	5.52	5.32	4.64	5.06
1.54	0.09	0.09	0.07	0.04	0.09	0.05	0.06	0.04	0.10
0.47	0.24	0.39	0.35	0.26	0.48	0.50	0.48	0.55	0.85
100.18	100.05	99.92	100.07	100.10	100.12	100.58	99.44	99.45	100.48
1026	379	490	1095	550	889	1313	664	773	988
23	10	30	17	25	10	7	2	16	
	16	8	6	26	15			12	
8	22	24	11	10	4	11	15	55	27
	25	30	17	28	7	4		32	
137	133	128	158	141	122	128	138	173	159
662	225	375	622	316	678	655	321	265	220
68	37	45	55	30	63	61	19	33	25
173	48	56	31	36	51	67	75	80	143
40	123	104	36	63	28	37	52	236	120
1082	507	515	518	362	705	886	818	288	526
0.88	0.98	0.95	1.00	1.00	1.01	0.95	0.99	0.94	0.94

31	32	33	34	35	36	37	38	39	40
GBH granite in area D							Leucosome		
03020304	**03020308**	**95020403**	**95020404**	**03020309**	**95020405**	**95020406**	**03020514**	**03020601**	**03020517**
74.25	74.61	75.40	75.52	75.84	76.53	76.73	71.63	72.03	72.96
0.13	0.26	0.11	0.12	0.21	0.11	0.12	0.32	0.23	0.09
14.63	13.21	13.65	13.20	12.45	13.04	12.84	14.81	14.97	15.20
0.69	0.72	0.40	0.81	1.13	0.47	0.50	0.80	0.36	0.16
0.59	1.25	0.56	0.58	1.01	0.41	0.49	0.69	0.30	0.27
0.03	0.33	0.28	0.35	0.08	0.25	0.28	0.34	0.25	0.06
0.01	0.03	0.00	0.01	0.01	0.01	0.01	0.03	0.01	0.00
0.81	1.16	0.85	0.88	0.72	0.81	0.83	1.24	0.80	0.55
3.14	2.83	3.37	2.80	2.74	2.99	3.24	2.51	2.65	2.25
5.95	5.69	5.73	6.01	5.44	5.78	5.33	7.88	8.29	8.85
0.03	0.03	0.02	0.01	0.05	0.01	0.02	0.06	0.06	0.01
0.33	0.54	0.29	0.37	0.38	0.29	0.32	0.45	0.44	0.36
100.58	100.65	100.67	100.67	100.06	100.70	100.70	100.76	100.38	100.76
304	728	234	237	318	455	151	2072	2204	3245
6		6	2		23	13	13	2	4
	4				1	1			
1	11	2	3	6	4	20	13	8	1
		20	23		22	28			
149	160	173	164	209	201	264	235	216	235
68	263	128	136	96	172	84	682	771	1739
28	10	13	4		2		56	40	49
22	93	27	34	76	30	73	73	57	27
11	30	11	9	46	17	16	18	11	2
186	494	130	144	340	218	196	243	35	75
1.12	1.02	1.03	1.04	1.06	1.03	1.02	0.99	1.01	1.06

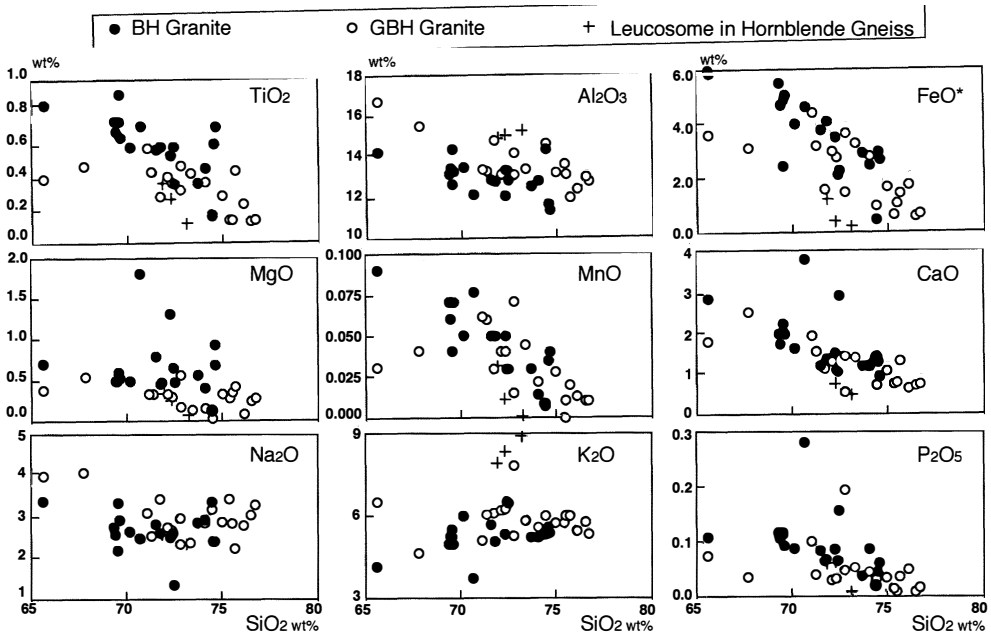

Fig. 5. Harker diagrams for major elements. $FeO^{*}=FeO+0.9Fe_2O_3$.

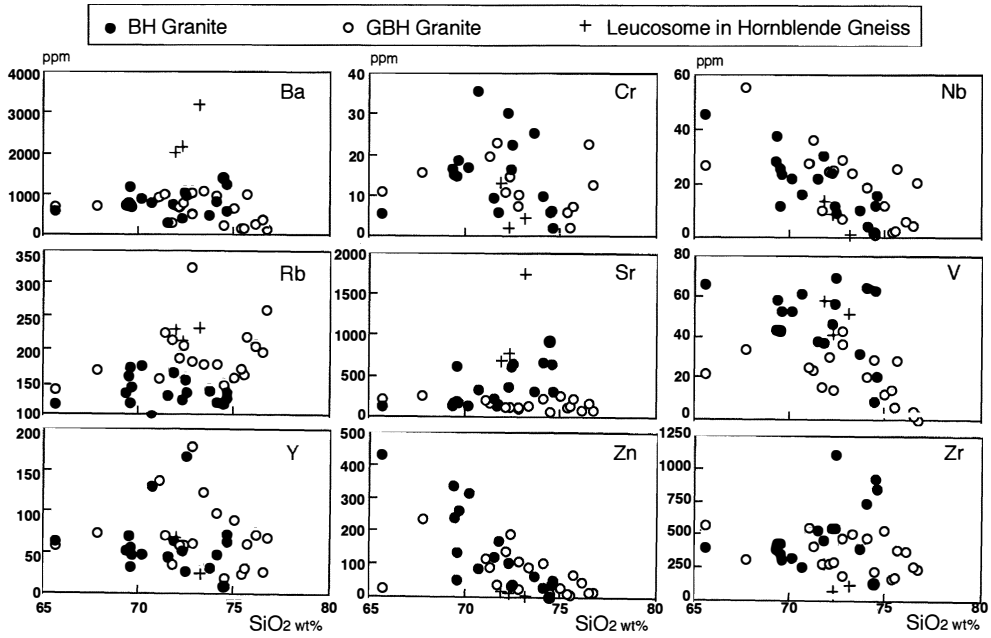

Fig. 6. Harker diagrams for trace elements.

5. Sr and Nd isotopic composition

5.1. *Analytical procedure*

Isotope analyses were performed with MAT 261-type (modified from MAT 260) and MAT 262-type mass spectrometers at Niigata University. Extraction procedures for Sr, Sm and Nd followed Kawano *et al*. (1999). Ratios of $^{87}Sr/^{86}Sr$ and $^{143}Nd/^{144}Nd$ were normalized to $^{86}Sr/^{88}Sr=0.1194$ and $^{146}Nd/^{144}Nd=0.7219$, respectively. The average $^{87}Sr/^{86}Sr$ ratio of NBS987 during this study was 0.710196 ± 0.000015 ($n=26$). The $^{87}Sr/^{86}Sr$ ratios in Table 2 were reported relative to NBS987 $=0.710251$ and the $^{143}Nd/^{144}Nd$ ratios were reported relative to 0.512115 (JNdi-1, Geological Survey of Japan standard sample) corresponding to 0.511858 of LaJolla (Tanaka *et al*., 2000). The blanks for the procedures were <0.14 ng of Rb, <0.99 ng of Sr, <0.03 ng of Sm and <0.26 ng of Nd. The age and initial $^{87}Sr/^{86}Sr$ ratio were calculated by the computer program of Kawano (1994) using the equation of York (1966) with the following decay constants: $\lambda^{87}Rb=1.42\times10^{-11}$/y (Steiger and Jäger, 1977) and $\lambda^{147}Sm=6.54\times10^{-12}$/y (Lugmair and Marti, 1978). Standard errors used for $^{87}Sr/^{86}Sr$ and $^{87}Rb/^{86}Sr$ ratios calculation were 0.015% and 5% respectively. We used the following Chondritic Uniform Reservoir ($=0$ Ma) for calculation of initial εSr and εNd values: $^{87}Sr/^{86}Sr=0.7045$, $^{87}Rb/^{86}Sr=0.0827$, $^{143}Nd/^{144}Nd=0.512638$, $^{147}Sm/^{144}Nd=0.1966$ (Goldstein *et al*., 1984).

5.2. *Whole rock isochron age*

The analytical results of the PSMGs and five metamorphic rocks in the Ongul Islands are listed in Table 2, and isochron diagrams for the granites from each area are shown in Fig. 7. Sample 03020512 collected from an isolated body in the western part of area A (Fig. 1) has a different mode of occurrence and geochemical characteristics from other samples (Table 1 and Figs. 5, 6) suggesting that it is unlikely to have been in equilibrium isotopically with them. Thus, this sample is excluded for calculation of the isochron age. Six whole rock samples from the BH granite in the eastern part of area A yielded an Rb-Sr whole rock isochron age of 580 ± 23 Ma with an initial $^{87}Sr/^{86}Sr$ ratio of 0.70784 ± 0.00059. Three leucosomes in the hornblende gneiss are plotted near and close to the 580 Ma isochron defined by the BH granites, and lie on a slightly steeper line than the isochron.

Shibata *et al*. (1985) reported the Rb-Sr mineral isochron age of 483 ± 10 Ma for gneissose granite (80EO125) in this area (Fig. 1; Shibata *et al*., 1986, Fig. 2). Sample 80EO125 is also plotted on the whole rock isochron of area A (Fig. 7), suggesting the isotopic data in this study is reproducible. Shibata *et al*. (1986) reported the Rb-Sr whole rock isochron age of 683 ± 13 Ma for metamorphic rocks in East Ongul Island. However, their samples were collected over a wide area of the island. Consequently, these samples were probably not homogeneous with respect to the Rb-Sr system. Shibata *et al*. (1986) pointed out that samples from a single outcrop yielded an Rb-Sr whole rock isochron age of 574 Ma, which is consistent with the isochron age obtained in this study. The errors of the age and initial ratio in the isochron of area A are relatively large; however, the isochron age is consistent with that of the migmatite and granite in the Breidvågnipa (576 Ma; Shimura *et al*., 1998), and both Rb-Sr whole rock

Table 2. Rb, Sr, Sm and Nd concentrations and $^{87}Sr/^{86}Sr$ and $^{143}Nd/^{144}Nd$ isotopic ratios.

No.	Sample No.	Rb (ppm)	Sr (ppm)	$^{87}Sr/^{86}Sr$ (2σ)	$^{87}Rb/^{86}Sr$	Sr ratio at 580 m.y. before present	εSr (580 Ma)	Sm (ppm)	Nd (ppm)	$^{143}Nd/^{144}Nd$ (2σ)	$^{147}Sm/^{144}Nd$	Nd ratio at 580 m.y. before present	εNd (580 Ma)
<BH granite in area A>													
2	95020204	139	145	0.73166(1)	2.78	0.70870	+62.0	-------	-------	-------	-------	-------	-------
3	95020206	164	172	0.73004(1)	2.76	0.70719	+40.9	-------	-------	-------	-------	-------	-------
4	95020203	177	199	0.72913(1)	2.58	0.70780	+49.8	14.77	68.83	0.512402(14)	0.130	0.511909	+0.4
6	95020101	147	183	0.72667(1)	2.33	0.70740	+43.6	-------	-------	-------	-------	-------	-------
7	03020603	102	335	0.71514(2)	0.88	0.70785	+49.3	-------	-------	-------	-------	-------	-------
8	95020205	181	140	0.73903(1)	3.75	0.70800	+52.7	12.3	57.1	0.512474(13)	0.130	0.511979	+1.7
10	03020512	121	926	0.70868(2)	0.38	0.70555	+16.9	0.95	5.74	0.512286(13)	0.100	0.511907	+0.3
<BH granite in area B>													
11	03020610	137	662	0.71292(1)	0.60	0.70796	+51.4	-------	-------	-------	-------	-------	-------
13	95020301	128	375	0.71795(1)	0.99	0.70977	+77.0	20.25	89.61	0.512435(9)	0.137	0.511916	+0.5
14	95020303	158	622	0.71303(1)	0.74	0.70695	+37.5	11.54	75.80	0.512231(14)	0.092	0.511881	-0.2
17	03020616	128	655	0.71136(1)	0.57	0.70669	+33.2	8.36	36.33	0.512438(14)	0.139	0.511909	+0.4
18	03020608	138	321	0.72472(1)	1.25	0.71442	+143	10.31	45.41	0.512375(12)	0.137	0.511853	-0.7
<GBH granite in area C>													
21	95020308	230	171	0.73972(1)	3.90	0.70743	+45.5	16.83	79.30	0.512439(13)	0.128	0.511953	+1.2
24	03020505	187	127	0.74615(3)	4.28	0.71079	+92.4	-------	-------	-------	-------	-------	-------
25	03020504	183	135	0.74565(1)	3.94	0.71309	+125	15.51	76.95	0.512383(14)	0.122	0.511920	+0.6
26	03020506	182	229	0.72652(2)	2.30	0.70746	+45.1	12.81	58.06	0.512396(14)	0.133	0.511889	0.0
27	95020305	221	226	0.72845(1)	2.83	0.70501	+10.9	15.62	62.28	0.512525(9)	0.152	0.511949	+1.1
<GBH granite in area D>													
29	95020402	220	140	0.76424(1)	4.57	0.72643	+315	10.40	57.20	0.512233(14)	0.110	0.511815	-1.5
30	03020307	329	115	0.83940(1)	8.38	0.77006	+937	-------	-------	-------	-------	-------	-------
32	03020308	160	263	0.72803(1)	1.76	0.71344	+130	17.45	86.29	0.512361(13)	0.122	0.511896	+0.1
35	03020309	209	96	0.81406(1)	6.36	0.76143	+812	-------	-------	-------	-------	-------	-------
36	95020405	201	172	0.75898(2)	3.40	0.73088	+378	2.70	9.74	0.512410(10)	0.168	0.511772	-2.3
<Leucosome in the hornblende gneiss in area A>													
38	03020514	235	682	0.71621(1)	1.00	0.70796	+53.0	-------	-------	-------	-------	-------	-------
39	03020601	216	771	0.71250(1)	0.81	0.70579	+22.0	9.40	43.94	0.512359(14)	0.129	0.511867	-0.5
40	03020517	235	1739	0.70731(1)	0.39	0.70408	-2.0	2.61	28.58	0.512142(13)	0.055	0.511932	+0.8
<Metamorphic rocks>													
	79022008*	29.7**	423**	0.70685(1)	0.20	0.70517	+10.0	0.78	3.81	0.512383(12)	0.124	0.511913	+0.4
	79022016*	3.98**	413**	0.70469(1)	0.03	0.70446	-0.5	5.33	22.16	0.512548(11)	0.145	0.511995	+2.0
	79100201*	9.5**	89.6**	0.70708(1)	0.31	0.70454	+0.8	1.65	6.40	0.512500(6)	0.156	0.511908	+0.3
	79100202*	9.9**	404**	0.70568(1)	0.07	0.70509	+8.6	3.57	13.90	0.512555(14)	0.155	0.511965	+1.5
	950205M6	79	957	0.70687(1)	0.24	0.70489	+6.9	5.77	41.85	0.512295(14)	0.083	0.511978	+1.7

No, sample numbers in Fig. 1; *, Same rock powder sample reported in Shibata et al. (1986); **, Data are cited from Shibata et al.(1986).

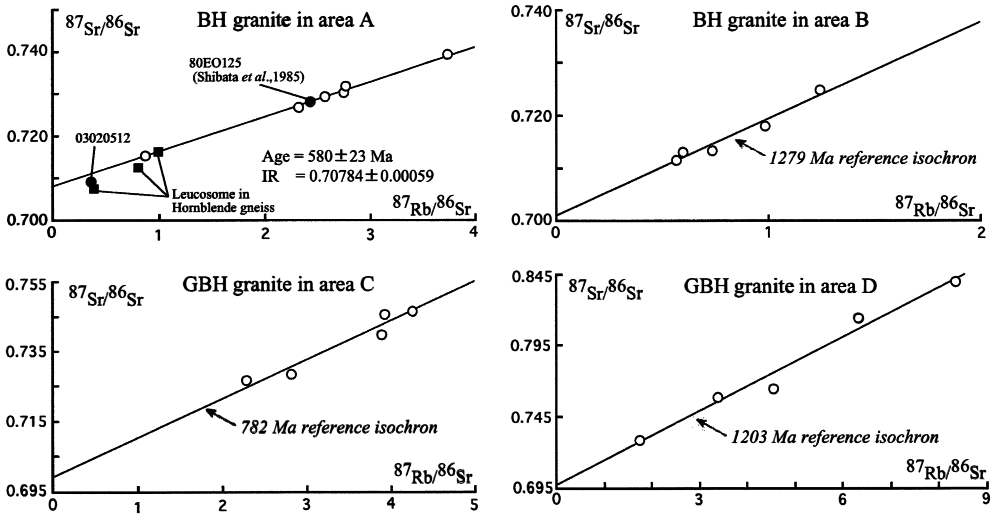

Fig. 7. Rb-Sr whole rock isochrons for the PSMGs. Solid symbols are excluded for calculation of the isochron ages.

isochron ages are slightly older than SHRIMP U-Pb zircon and CHIME monazite ages (Shiraishi *et al*., 1994; Asami *et al*., 1997).

BH granite in area B, and GBH granites in areas C and D give Rb-Sr whole rock isochron ages of 1279 Ma, 782 Ma and 1203 Ma with initial Sr isotopic ratios of 0.70087, 0.69905 and 0.69723, respectively. They are pseudo-isochrons, because the isotopic data of those areas are apparently scattered (Fig. 7) and errors of isochron ages are more than 200 Ma; their initial $^{87}Sr/^{86}Sr$ ratios have very low values for terrestrial rocks and meteorites.

Sm-Nd data of the PSMGs from all areas do not define an isochron, because they show small variation in the system (Table 2) and also are scattered on the isochron diagrams.

5.3. Initial εSr and εNd values for the PSMGs

εSr and εNd values at 580 m.y. before the present (εSr_{580Ma} and εNd_{580Ma}) are calculated to determine the petrogenesis of the PSMGs. εSr_{580Ma} values of the BH granite range from +17 to +143, while those of the GBH granite vary widely from +11 to +1165. εNd_{580Ma} values of the BH granite also have a relatively narrow range in comparison with those of the GBH granites, which have the lowest εNd_{580Ma} value of −2.3 (Table 2). εSr and εNd values of the leucosome at 580 m.y. before present range from −2.0 to +53.2 for Sr and −0.5 to +0.8 for Nd, respectively. Those of metamorphic rocks vary between −0.5 and +10 for Sr, and +0.3 to +2.0 for Nd (Table 2). εSr_{580Ma} values of leucosomes and metamorphic rocks are slightly lower than those of BH and GBH granites.

The relation of εSr_{580Ma} and εNd_{580Ma} values of the PSMGs with the mafic to intermediate metamorphic rocks is illustrated in Fig. 8. The BH and GBH granites

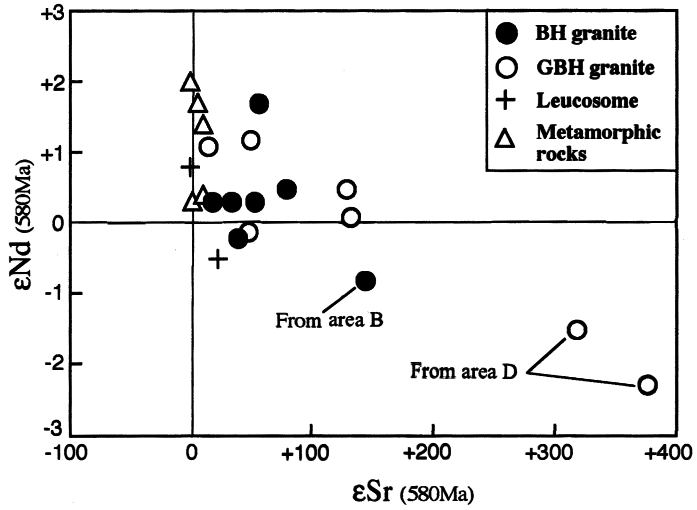

Fig. 8. εSr_{580Ma} *versus* εNd_{580Ma} *diagram.*

extend from quadrant I to quadrant IV, implying that their magmas contain mixtures of Sr and Nd derived from sources in the mantle in quadrant II and the continental crust in quadrant IV. The GBH granite especially shows conspicuously large values of εSr_{580Ma}. Furthermore, two samples from the D area indicate εSr_{580Ma} values more than +800 (Table 2). The field of the BH granite overlaps with that of the GBH granite, and the metamorphic rocks are plotted close to that of the BH granite. The leucosomes are also plotted near the field of the BH granite.

6. Discussion

6.1. Interpretation of the Rb-Sr isochron age

We obtain the Rb-Sr whole rock isochron age of 580 Ma from the BH granite area A; however, it is slightly older than the SHRIMP U-Pb zircon and CHIME Th-U-Pb monazite ages (Shiraishi *et al*., 1994; Asami *et al*., 1997). The closure temperature of the Rb-Sr whole rock system for felsic rocks has been stated as *ca.* 700°C (*e.g.* Harrison *et al*., 1979). However, if the rock is heated again at *ca.* 700°C, its Sr isotopic composition would not be homogenized totally. Kagami *et al*. (2003) pointed out that it seems to be difficult to attain regional Sr homogenization without activity of magma or fluid, even under metamorphism at a lower crustal level. Dickin (1995) also emphasized that isotopic equilibrium in the Rb-Sr whole rock system was not attained under metamorphism even during a high temperature condition. The Rb-Sr data of the granites and gneissose rocks in the Ongul Islands do not define a single isochron (Fig. 7, Table 2). This fact suggests that even if the rocks in the islands were heated to over 800°C by metamorphism, they could not have attained Sr isotopic homogenization. Moreover, there is no evidence of effective interaction between granites and fluid in area A; therefore, the Rb-Sr whole rock isochron age of 580 Ma obtained from the BH

granite is interpreted as the igneous active age.

6.2. Estimated source materials for the PSMGs

The pre/syn-metamorphic granites in the Breidvågnipa are considered to have been derived from pelitic gneiss by partial melting, because they are peraluminous composition, having ASI of 1.02 to 1.11 and a high initial Sr ratio of 0.7102 (Shimura *et al.*, 1998). The initial Sr ratio $_{(580Ma)}$ of BH granite in area A is distinctly lower than that of granite in the Breidvågnipa, indicating that the pelitic metamorphic rock is not an appropriate source material for BH granite. Nishi *et al.* (2002) reported an initial Sr ratio of 0.70556 for hornblende biotite gneiss in Oku-iwa Rock, Prince Olav Coast, and estimated that the protolith of the gneiss consisted of intermediate igneous rocks based on their chemical compositions. Shibata *et al.* (1986) obtained an initial Sr ratio of 0.7050 from mafic granulites in a single outcrop in East Ongul Island. In this study, Sr ratios at 580 m.y. before present of metamorphic rocks (biotite orthopyroxene amphibolite, biotite hornblende orthopyroxene gneiss, orthopyroxene granulite, orthopyroxene hornblende granulite and pyroxene gneiss) range from 0.70446 to 0.70517 (Table 2). This fact suggests that these metamorphic rocks originated from mafic to intermediate igneous rocks. The initial Sr ratio $_{(580Ma)}$ of BH granite in area A is higher than those of mafic to intermediate metamorphic rocks. Sr ratios at 580 m.y. before present of leucosomes in hornblende gneiss are slightly lower than those of BH granite, indicating different chemical features from the BH granite (Figs. 5 and 6), and are not plotted on the Rb-Sr isochron (Fig. 7), implying that source magma for BH granite might not have directly originated by partial melting of hornblende gneiss in the Island. There is, however, a possibility that source magma derived from mafic to intermediate metamor-

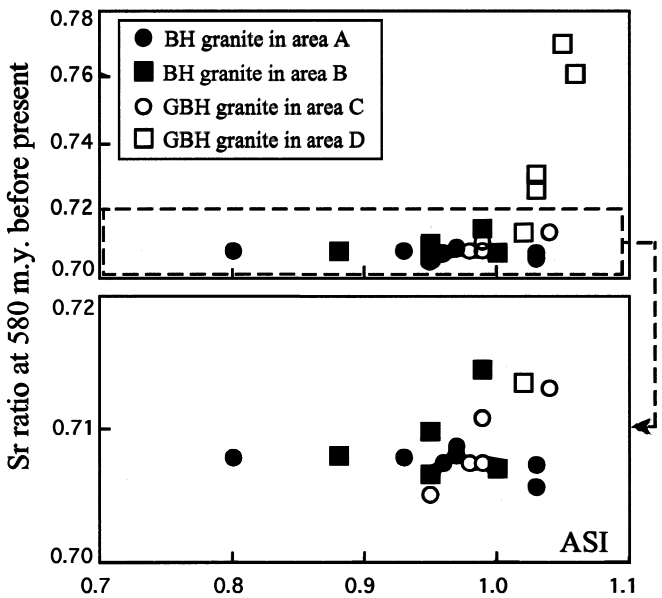

Fig. 9. Sr isotopic ratio at 580 m.y. before present versus ASI (aluminum saturation index) diagram.

phic rocks was affected by old continental crust, because isotopic compositions of the PSMGs indicate extension to lower right quadrant in the ε diagram (Fig. 8). BH granite in area B and GBH granites might be more influenced by crustal materials than those in area A (Fig. 8).

BH granite in area B and GBH granites in areas C and D do not indicate any clear isochron (Fig. 7). The arrangements of these granites are steeper than the isochron of 580 Ma (Fig. 7), suggesting a possibility that they were influenced by materials with high $^{87}Sr/^{86}Sr$ and $^{87}Rb/^{86}Sr$ ratios. Moreover, Sr ratios at 580 m.y. before present *vs.* ASI relations of the PSMGs are illustrated in Fig. 9. Sr ratios at 580 m.y. before present of the BH granite in area A indicate horizontal change with increasing ASI, whereas the ratios of BH granite in area B and GBH granites increase with increasing ASI, suggesting that the latter granites were more affected by material with high ASI than the former granite.

It is likely that the PSMGs were originated by mixing between magma derived from mafic to intermediate metamorphic rocks and old continental crust with high ASI, $^{87}Sr/^{86}Sr$ and $^{87}Rb/^{86}Sr$ ratios.

Acknowledgments

The authors are grateful to all members of JARE-36 and -44. Special thanks are due to M. Arita (Attached High School of Hiroshima University), K. Naito (Geological Survey of Japan), T. Ikeda (Kyushu University), T. Kawakami (Geological Survey of Japan) and T. Kawasaki (Ehime University) for their collaboration in the field work. The authors are indebted to Y. Osanai (Kyushu University; Fukuoka University of Education at the time) and S. Kakubuchi (Saga University) for XRF analysis. We also would like to express our thanks to T. Hokada (NIPR) for EPMA analysis. Thanks are also due to K. Shiraishi (NIPR) and M. Yuhara (Fukuoka University) for their valuable comments on the draft. We acknowledge T. Miyamoto (Kyushu University), A. Kamei (Shimane University) and an anonymous reviewer for their critical reviews of the manuscript. Part of this work was supported by a Grant-in-Aid for Scientific Research of the Ministry of Education, Japan to Y.K. (No. 07740427).

References

Ajishi, H., Kawano, Y., Kawakami, T. and Ikeda, T. (2004): Geochronological study of post-metamorphic granite from Kasumi Rock, Lützow-Holm Complex, East Antarctica. Polar Geosci., **17**, 35–44

Asami, M., Suzuki, K. and Adachi, M. (1997): The U and Pb analytical data and CHIME dating of monazites from metamorphic rocks of the Rayer, Lützow-Holm, Yamato-Bergica and Sør Rondane complexes, East Antarctica. Proc. NIPR Symp. Antarct. Geosci., **10**, 130–152.

Dickin, A.P. (1995): Radiogenic Isotope Geology. Cambridge, Cambridge Univ. Press, 490 p.

Goldstein, S.L., O'Nions, R.K. and Hamilton, P.J. (1984): A Sm-Nd study of atmospheric dusts and particulates from major river systems. Earth Planet. Sci. Lett., **70**, 221–236.

Harrison, T.M., Armstrong, R.L., Naeser, C.W. and Harakal, J.E. (1979): Geochronology and thermal histry of the Coast Plutonic Complex, near Prince Rupert, British Columbia. Can. J. Earth Sci., **16**, 400–410.

Hiroi, Y. and Onuki, H. (1985): Hornblende gneisses from Syowa Station, East Antarctica. Mem. Natl. Inst. Polar Res., Spec. Issue, **37**, 63–81.

Hiroi, Y., Shiraishi, K. and Motoyoshi, Y. (1991): Late Proterozoic paired metamorphic complexes in East Antarctica, with special reference to the tectonic significance of ultramafic rocks. Geological Evolution of Antarctica, ed. by M.R.A. Thomson *et al.* Cambridge, Cambridge Univ. Press, 83–87.

Ishikawa, M., Shiraishi, K., Motoyoshi, Y., Tsuchiya, N., Shimura, T. and Yanai, K. (1994): Explanatory text of geological map of Ongul Islands, Lützow-Holm Bay, Antarctica. Antarctic Geol. Map Ser., Sheet 36. Tokyo, Natl. Inst. Polar Res.

IUGS Subcommision (1973): Plutonic rocks. Classification and nomenclature recommended by the IUGS Sub-commision on the Systematics of Igneous Rocks. Geotimes, **18** (10), 26–30.

Kagami, H., Shimura, T., Yuhara, M., Owada, M., Osanai, Y. and Shiraishi, K. (2003): Resetting and closing condition of Rb-Sr whole-rock isochron system: some samples of metamorphic and granitic rocks from the Gondwana super-continent and Japan Arc. Polar Geosci., **16**, 227–242.

Kawano, Y. (1994): Calculation program for isochron ages of Rb-Sr and Sm-Nd systems, using personal computer. Geoinformatics, **5**, 13–19 (in Japanese with English abstract).

Kawano, Y., Nishi, N. and Ishisaka, T. (1999): Preparation of samples for Sr and Nd isotopic analysis at petrochemical laboratory. J. Fac. Cul. Edu. Saga Univ., **4**, 139–146 (in Japanese with English abstract).

Kizaki, K. (1962): Structural geology and petrology of the East Ongul Island, East Antarctica. Part I. Structural geology. Nankyoku Shiryô (Antarct. Rec.), **14**, 27–35.

Kizaki, K. (1964): Tectonics and petrography of the East Ongul Island, Lützow-Holm Bukt, Antarctica. JARE Sci. Rep., Ser. C (Geology), **2**, 1–24.

Lugmair, G.W. and Marti, K. (1978): Lunar initial $^{143}Nd/^{144}Nd$: differential evolution of the lunar crust and mantle. Earth Planet. Sci. Lett., **39**, 349–357.

Nishi, N., Kawano, Y. and Kagami, H. (2002): Rb-Sr and Sm-Nd isotopic geochronology of the granitoid and hornblende biotite gneiss from Oku-iwa Rock in the Lützow-Holm Complex, East Antarctica. Polar Geosci., **15**, 46–65.

Shibata, K., Yanai, K. and Shiraishi, K. (1985): Rb-Sr mineral isochron ages of metamorphic rocks around Syowa Station and from the Yamato Mountains, East Antarctica. Mem. Natl. Inst. Polar Res., Spec. Issue, **37**, 164–171.

Shibata, K., Yanai, K. and Shiraishi, K. (1986): Rb-Sr whole-rock ages of metamorphic rocks from eastern Queen Maud Land, East Antarctica. Mem. Natl. Inst. Polar Res., Spec. Issue, **43**, 133–148.

Shimura, T., Fraser, G.L., Tsuchiya, N. and Kagami, H. (1998): Genesis of the migmatites of Breidvågnipa, East Antarctica. Mem. Natl. Inst. Polar Res., Spec. Issue, **53**, 109–136.

Shiraishi, K., Hiroi, Y., Ellis, D.J., Fanning, C.M., Motoyoshi, Y. and Nakai, Y. (1992): The first report of a Cambrian orogenic belt in East Antarctica—An ion microprobe study of the Lützow-Holm Complex. Recent Progress in Antarctic Earth Science, ed. by Y. Yoshida *et al*. Tokyo, Terra Sci. Publ., 67–73.

Shiraishi, K., Ellis, D.J., Hiroi, Y., Fanmng, C.M., Motoyoshi, Y. and Nakai, Y. (1994): Cambrian orogenic belt in East Antarctica and Sri Lanka: Implications for Gondwana assembly. J. Geol., **102**, 47–65.

Shiraishi, K., Hokada, T., Fanning, C.M., Misawa, K. and Motoyoshi, Y. (2003): Timing of thermal events in eastern Dronning Maud Land, East Antarctica. Polar Geosci., **16**, 76–99.

Steiger, R.H. and Jäger, E. (1977): Subcommission on geochronology: Convention on the use of decay constants in geo- and cosmo-chronology. Earth Planet. Sci. Lett., **36**, 359–362.

Tanaka, T., Togashi, S., Kamioka, H., Amakawa, H., Kagami, H. and other 14 authors (2000): JNdi-1: a neodymium isotopic reference in consistency with LaJolla neodymium. Chem. Geol., **168**, 179–181.

Windley, B.F. (1995): The Evolving Continents, 3rd ed. J. Wiley, 526 p.

Yanai, K., Kizaki, K., Tatsumi, T. and Kikuchi, T. (1974a): Geological map of East Ongul Island, Antarctica. Antarct. Geol. Map Ser., Sheet I (with explanatory text 13 p.). Tokyo, Natl. Inst. Polar Res.

Yanai, K., Tatsumi, T. and Kikuchi, T. (1974b): Geological map of West Ongul Island, Antarctica. Antarct. Geol. Map Ser., Sheet 2 (with explanatory text 5 p.). Tokyo, Natl. Inst Polar Res.

York, D. (1966): Least squares fitting of a straight line. Can. J. Phys., **44**, 1079–1086.